Earth Reinforcement, Ochiai, Yasufuku & Omine (eds) © *1996 Balkema, Rotterdam. ISBN 90 5410 833 9*

Deep seated stability of soil nailing walls

S. Bang & B. F. Wilkins
Department of Civil and Environmental Engineering, South Dakota School of Mines and Technology, Rapid City, S.Dak., USA
C.K. Shen
Department of Civil and Structural Engineering, Hong Kong University of Science and Technology, Hong Kong

ABSTRACT: An approximate solution to evaluate the factor of safety of soil nailing walls against the deep-seated failure has been developed. It was added to the existing solution method, which analyzes the stability of soil nailing walls based on the limiting equilibrium of driving and resisting forces along the assumed potential failure surface that passes through the toe of the wall. The developed soil nailing wall stability analysis method has been applied to identify the effects of the soil nailing wall geometry, soil strength, nail length, and depth of bedrock on the failure mechanism. Specifically, the magnitude of the soil nailing wall slope angle when the dominant failure mechanism changes from deep-seated failure to toe failure has been looked into.

1 FUNDAMENTALS

An extensive study of the soil nailing wall including the design and analysis methods has been conducted by the writers (Bang, 1980, Bang et al. 1993, Shen et al. 1981a, 1981b, 1981c, 1982). The design approach is based on the assumption that the potential failure surface can be represented by a parabolic curve passing through the toe of the wall. This assumption has been derived from the results of a finite element study of soil nailing model walls tested inside a centrifuge (Shen 1982). A classical method of equilibrium analysis is then used to evaluate the stability of the soil nailing wall by considering the contribution of the nails to the overall stability. The tensile forces developed in the reinforcing nails are divided into tangential and normal components along the assumed failure plane. The maximum tensile force in each reinforcing nail is calculated and compared with the tensile resistance of the nails to identify the possibility of nail yielding. The overall minimum factor of safety is then obtained by considering a series of parabolic potential failure surfaces.

2 DEEP SEATED SLOPE STABILITY

The factor of safety describes in the previous section is based on the sliding mechanism whose failure surface passes through the toe of the soil nailing wall. This is a reasonable and correct mechanism for relatively steep walls. However, for walls with relatively flat slope angles, the failure surface may penetrate below the toe of the wall.

For the purpose of analyzing the stability of soil nailing walls that include a deep-seated failure surface, circular failure surfaces have been assumed. The minimum factor of safety against the deep-seated failure can then be calculated from the ratio between the resisting moment and the overturning moment about the circle center, considering a series of circles that may or may not intersect with the soil nails.

The overturning moment associated with a given failure circle can be approximated from the method described by Lowe (Lowe, 1989). The Lowe's method calculates the minimum factor of safety against overturning for slopes with no reinforcement, no surcharge, and level ground surface. To approximately estimate the factor of safety against the deep-seated failure of a soil nailing wall that may have surcharge and/or sloping ground surface, the following steps have been taken.

First, the minimum factor of safety against the deep-seated failure and the corresponding overturning moment are calculated from the Lowe's method, assuming no surcharge and level ground surface. The center of the circular failure surface that contains the toe of the slope within it, i.e., the deep-seated failure, of a homogeneous slope lies along the vertical line passing through the mid-slope of the embankment. The resulting factor of safety is expressed as

$$FS_D = N_1 \frac{C_u}{\gamma H} + N_2 \left[\frac{C_m}{\gamma H} + \lambda \tan\phi_m \right] \qquad (1)$$

where λ, N_1 and N_2 are constants defined by Lowe, which depend on the angle (β) and height (H) of the slope and the depth to the bottom of the circle from the embankment toe. C_u, C_m, and ϕ_m are the undrained shear strength of the foundation soil, cohesion of the embankment soil, and the friction angle of the embankment soil, respectively. γ is the unit weight of the embankment soil. The minimum factor of safety (FS_{min}) is obtained through a search of the critical circle by varying the depth to the bottom of the circle from the toe of the embankment (D). The undrained shear strength of the foundation soil can vary linearly with depth. The overturning moment (M_o) associated with a given circular arc is expressed as

$$M_o = \left[y\left(D + \frac{H}{2}\right) - 0.5\left(D + \frac{H}{2}\right)^2 - \frac{H^2}{24} - \frac{\ell^2}{24} \right] \gamma H \quad (2)$$

where ℓ is the horizontal extent of the sloping portion of the embankment, i.e., $H \cot\beta$.

Once the minimum factor of safety and the overturning moment are calculated, the corresponding resisting moment (M_R) can be obtained from the definition of the factor of safety, i.e.,

$$M_R = FS_{min} M_o \qquad (3)$$

The calculated overturning moment however needs to be modified due to the existence of the sloping ground surface, surface distributed surcharge, and surface point loads. They are calculated individually, considering the material and geometric details, and added to obtain the modified overturning moment (M_O').

Next, the calculated resisting moment is modified. In case when the assumed circular failure surface completely contained the entire soil nails, no modification is necessary, i.e., the calculated resisting moment from the Lowe's method is used directly. If the assumed circular failure surface intersects one or more soil nails, additional resisting moment (M_{R_1}) due to the resistance provided by the portions of soil nails located outside the failure surface needs to be considered. For each nail, the additional friction due to the overburden and surface loading is obtained individually by calculating the normal and shear stresses developed along the effective length of the nail. The modified resisting moment (M_R') is then calculated by adding the resisting moment obtained from Eq. (3) and the summation of individual additional resisting moment of each nail which is obtained by multiplying the additional frictional resistance with the moment arm from the center of the assumed failure circle, i.e.,

$$M_R' = M_R + M_{R_1} \qquad (4)$$

Finally, the factor of safety against the deep-seated failure (FS') of the soil nailing wall is calculated from

$$FS' = \frac{M_R'}{M_O'} \qquad (5)$$

The details of the formulation are not included in this paper. The calculations of the average shear strength of a layered soil system, the friction developed on each nail beyond the assumed failure surface, the stress distribution due to the surface loading, and the contribution of the sloping ground surface are essential parts of the formulation.

3 PARAMETRIC STUDY

The main objective of this study is to investigate the effects of various parameters that define a soil nailing wall on the factor of safety against the toe failure (FST) and the factor of safety against the deep seated failure (FSD). Specifically, it is intended to establish general conclusions concerning the role of various soil and geometric parameters in determining the dominant failure mechanism, e.g., deep-seated or toe failure.

3.1 Test Parameters and Results

The parametric study centered primarily on the effects of the slope angle and height of the soil nailing wall which define the boundary between the toe and deep-seated failure. Therefore, a typical soil nailing wall with a backfill of cohesive, frictionless soil underlain by like material was considered to eliminate the effect of the foundation soil on the factor of safety. Five soil and geometric parameters were selected as variables, as detailed below. The soil parameters that were held constant are also given.

Constants:
Soil unit wt.= 18.06 kN/m^3
Soil friction angle = 0°

Variables:
Soil cohesion = 47.88 and 95.76 kPa
Slope angle = 30, 45, 60, 75 degrees
Slope height (H) = 4.57, 9.14, 13.72, and 18.29 m
Nail length = 0.75 H, 1.0 H, and 1.25 H
Depth from toe to bedrock = 10.67, 13.72, and 18.29 m.

Figs - 1 through 4 show typical results of the factors of safety against the toe failure (FST) and the deep-seated failure (FSD) for various slope angles and nail lengths of soil nailing walls with given height and soil cohesion. Figure legends indicate the length of the soil nails as a multiple of the slope height (H). Figs - 5 through 8 show typical results of the factors of safety against the toe failure and the deep-seated failure for various wall heights and nail lengths for soil nailing walls with given slope angle and depth to bed rock. Thick and thin solid lines in the figures indicate results with backfill soil cohesion of 47.88 kPa and 95.76 kPa, respectively.

3.2 Effect of Soil Cohesion

Observations of Figs - 1 through 8 indicate that as the soil cohesion increases, the factor of safety also increases. When the soil cohesion is doubled the factor of safety is also doubled. It is noted that the intersection of FST and FSD curves in figures defines the slope angle (Figs - 1 through 4) or height (Figs - 5 through 8) at which the governing failure mode changes. For instance, in Fig - 5, for a

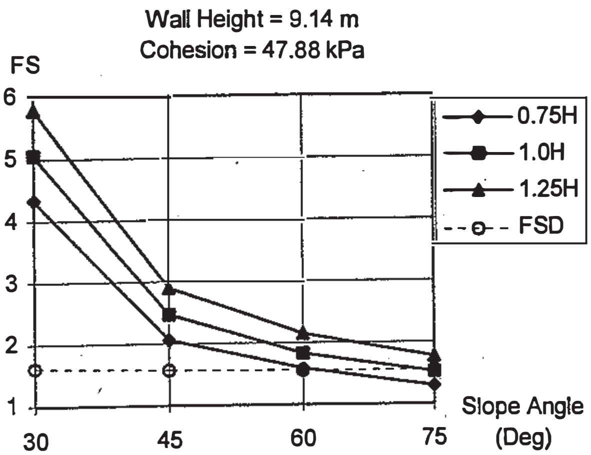

Fig - 1 Effect of Slope Angle on Factor of Safety - 1

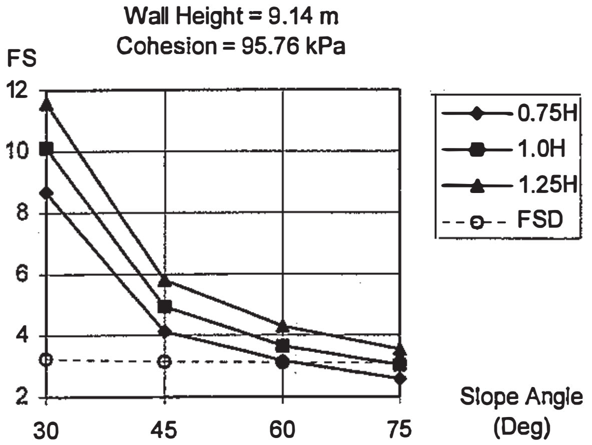

Fig - 2 Effect of Slope Angle on Factor of Safety - 2

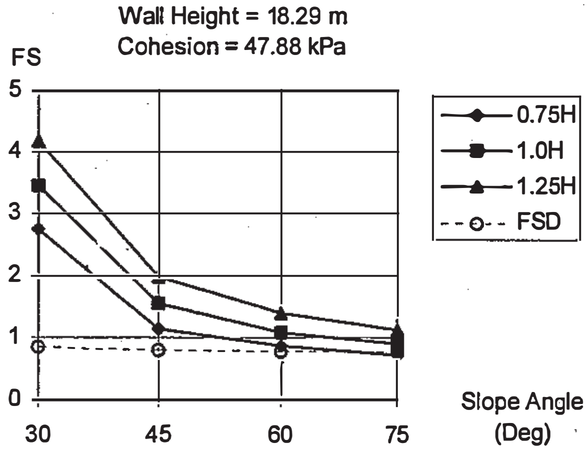

Fig - 3 Effect of Slope Angle on Factor of Safety - 3 slope with an angle of 15 degrees, depth to bedrock of 18.29 m, soil cohesion of 95.76 kPa, and nail length of 1.0 H, the dominant failure mechanism changes from the deep-seated to toe failure as the slope height exceeds approximately 10 meters. Fig - 1 indicates that the transition of failure mechanism occurs at the slope angle of 60 degrees for the soil nailing wall with a height of 9.14 m, cohesion of 47.88 kPa, and nail length of 0.75 H.

It is noted from all figures that the intersection points of FST and FSD do not change with variances in cohesion. This indicates that, although a variance in the value of cohesion directly effects FST and FSD, it does not have a significant effect on the slope angle or height at which the failure mode transition occurs.

3.3 Effect of Depth to Bedrock

Observations of Figs - 1 through 4 indicate that FSD is relatively insensitive to the depth to bedrock. There is a slight increase in FSD for higher and flatter slopes as the depth to bedrock decreases. However, the observed maximum increase in FSD is insignificant.

3.4 Effect of Slope Angle

As shown in Figs - 1 through 4, FST decreases as the slope angle increases. The rate of change in FST is relatively constant in the interval of 45 to 75 degrees. However, for slope angles less than 45 degrees, FST changes at a significantly higher rate.

As might be expected, FSD is less affected by the slope angle than FST. The change of slope angle from 30 to 75 degrees, for a given slope height, results in an increase of FSD ranging from 1% to 8%. The higher the slope height, the greater is the observed change in FSD due to the change in slope angle.

3.5 Effect of Wall Height

From Figs - 5 through 8 it is observed that as the wall height increases, both FST and FSD decrease as a result of increase in driving force of the soil mass. It is interesting to note that FST and FSD curves in the figures have similar shapes, with a higher rate of decrease in the interval of 4.57 to 9.14

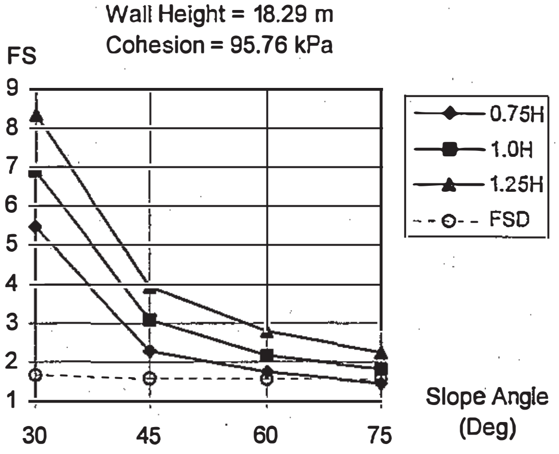

Fig - 4 Effect of Slope Angle on Factor of Safety - 4

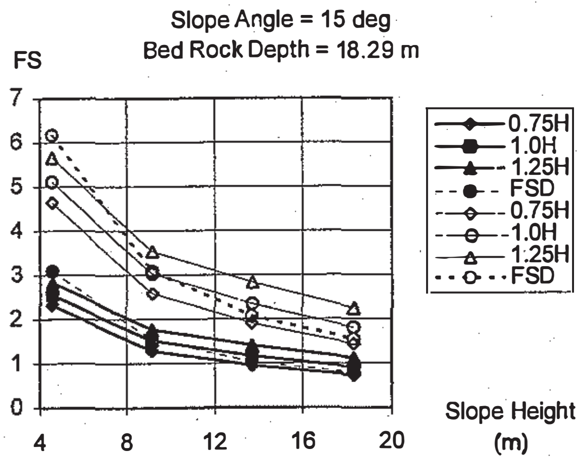

Fig - 5 Effect of Wall Height on Factor of Safety - 1

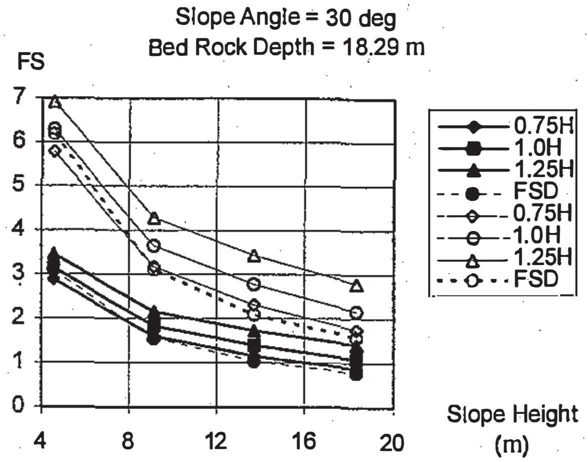

Fig - 6 Effect of Wall Height on Factor of Safety - 2

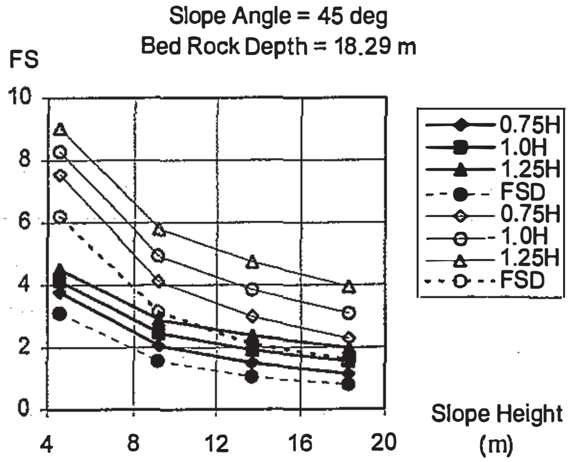

Fig - 7 Effect of Wall Height on Factor of Safety - 3

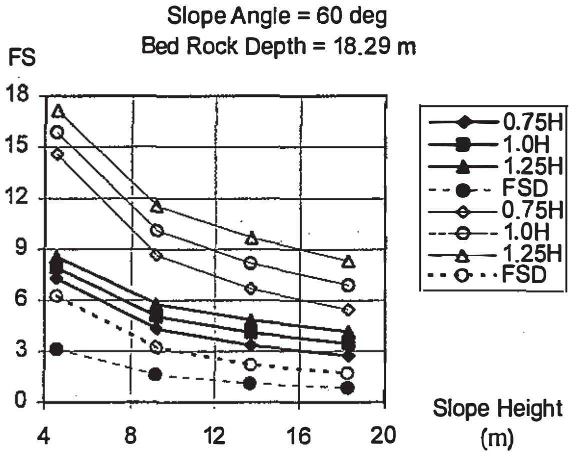

Fig - 8 Effect of Wall Height on Factor of Safety - 4

m than in subsequent intervals. Within the slope height interval of 4.57 to 9.14 m, FST decreases approximately 50%, whereas in the interval of 9.14 to 18.29 m FST decreases by approximately 25%.

Based on the observations described above, it may be concluded that as the slope height increases FST decreases with a decreasing rate.

3.6 Effect of Nail Length

It is obvious that, as the amount of reinforcement of a given slope increases, FST inherently increases also. This concept is correctly observed in this study as indicated in all figures. FST is noted to have increased from 17% to 74% (depending on the slope angle and the wall height) as the nail length increases from 0.75H to 1.25H. The average percentage increase in FST due to the nail length increase for wall heights of 4.57, 9.14, 13.72, and 18.29 m are 20, 37, 50, and 61%, respectively. It is observed that FST is significantly influenced by the nail length and that the percentage influence is more pronounced as the height of the slope increases. The results also indicate that the nail length has virtually no effect on FSD.

3.7 Transition Slope Angle

Figs - 1 through 4 clearly indicate that the addition of soil nails results in a steepened slope angle at which the transition of failure mode occurs. Table - 1 summarizes this transition slope angle for various wall heights and nail lengths of soil nailing walls with soil cohesion of 47.88 kPa and the depth to bed rock of 18.29 m..

Table 1. Transition slope angles

Wall height (m)	Nail length (m)	Transition slope angle (deg)
4.57	3.43.	57
4.57	4.57	61
4.57	5.72	69
9.14	6.86	61
9.14	9.14	75
9.14	11.43	-
13.72	10.29	69
13.72	13.72	-
13.72	17.15	-
18.29	13.72	71

For instance, when the wall height is 4.57 m and the nail is 3.43 m long, toe failure becomes a dominant failure mechanism when the slope angle is greater than 57 degrees. For angles less than 57 degrees, deep-seated failure is likely. Note that this value is slightly greater than the transition slope angle of non-reinforced homogeneous slopes, i.e., 53 degrees. The table indicates that as the nail length increases the transition slope angle increases also. This would be expected, as the additional nail length provides increased support against the toe failure. The transition slope angle also increases as the wall height increases.

4 CONCLUSIONS

The transition slope angle at which the failure mode transition occurs is significantly affected by the inclusion of soil nails. Inclusion of soil nails effectively increases FST, thereby allowing a steeper slope angle before FSD begins to govern the failure mode.

The addition of soil nails also allows a higher slope to be constructed while maintaining a given FST. As a result of increasing the slope height, FSD decreases and will therefore be more likely to control the mode of possible failure.

In general, the transition slope angle of the soil nailing wall is greater than that of the non-reinforced slope. The difference in the transition slope angle between the non-reinforced slopes and slopes reinforced with soil nails become greater as the slope height and/or the nail length increases.

It is observed as expected that FSD is more sensitive to the wall height than to the slope angle. The results also indicate that the transition slope angle is relatively unaffected by the change in soil cohesion.

The study described in this paper is limited in its scope; limited ranges of values of the wall height, slope angle, nail length, soil properties, and depth to bed rock have been considered. Therefore the results of this study may not be generalized for soil nailing walls with properties other than considered. Further in-depth study needs to be conducted for this purpose.

REFERENCES

Bang, S., C. K. Shen, and K. M. Romstad, "Analysis of an Earth-Reinforcing System for Deep Excavation," *Transportation Research Record* No. 749, 1980.

Bang, S., C. K. Shen, J. Kim, and P. P. Kroetch, "Investigation of Soil Nailing Systems," *Transportation Research Record,* No. 1269, 1993.

Low, B. K., "Stability Analysis of Embankments on Soft Ground," *ASCE*, Vol. 115, No. 2, Feb., 1989.

Shen, C. K., L. R. Herrmann, K. M. Romstad, S. Bang, Y. S. Kim, and J. S. DeNatale, "An In Sit Earth Reinforcement Lateral Support System," Report No. 81-03, University of California, Davis, A Report prepared for National Science Foundation, 1981.

Shen, C. K., S. Bang, and L. R. Herrmann, "Groun Movement Analysis of an Earth Support System," *ASCE*, Vol. 107, GT12, Dec., 1981.

Shen, C. K., S. Bang, K. M. Romstad, L. Kulchin, and J. S. DeNatale, "Field Measurements of an Earth Support System," *ASCE*, Vol. 107, GT12, Dec., 1981.

Shen, C. K., Y. S. Kim, S. Bang, and J. F. Mitchell "Centrifuge Modeling of Lateral Earth Support, *ASCE*, Vol. 108, GT9, 1982.